23

Achievements and Open Issues Toward Embedding Tactile Sensing and Interpretation into Electronic Skin Systems

Ali Ibrahim, Luigi Pinna, Lucia Seminara, and Maurizio Valle

Electrical, Electronic and Telecommunications Engineering, Department of Naval, via Opera Pia 11A, 16145 Genoa, Italy

23.1 Introduction

The development of the electronic skin (e-skin) is a very challenging goal that should be tackled from a system perspective.

The e-skin is usually intended as a hybrid stack-wise arrangement that incorporates tactile sensing (structural and functional materials, signal conditioning and acquisition, signal processing) and interpretation. Sensory inputs similar (but not limited) to those possessed by humans are essential to provide the necessary feedback to explore the environment and interact with objects.

A specific example of this general structure is shown in Figure 23.1 (adapted from Ref. [1]).

The *bottom layer* (*substrate*) is made of a structural material that can be rigid (e.g., the robot mechanical structure) or soft. Next layer (electronic layer) *hosts the electronic circuits*. Conventional electronics is typically integrated on very hard and flat (brittle) surfaces. Here the need is to conform to curved surfaces, requiring flexibility but also stretchability, to a certain extent, to follow all movements and deformations of the parts into which the electronic layer is integrated. The adoption of a flexible substrate does not necessarily guarantee the flexibility of the entire electronic circuit, as a too dense or not well-organized layout may drastically limit the flexibility of the overall structure. Also, system flexibility does not imply stretchability. In fact, even if the substrate is stretchable, the routing lines are intrinsically not, unless a dedicated design is adopted. Some interesting concepts are related to the creation of compliant and stretchable interconnections [2,3] and a very widespread approach to materials and mechanics for stretchable electronics is contained in a complete overview [4]. Requirements on conformability and stretchability put severe constraints on the reliability of the electronics, as mechanical stress on the electronic circuits can cause faults on interconnections and circuits. The counteraction can be at a material level; for what concerns this review, we will focus on increasing

Material-Integrated Intelligent Systems: Technology and Applications, First Edition.
Edited by Stefan Bosse, Dirk Lehmhus, Walter Lang, and Matthias Busse.

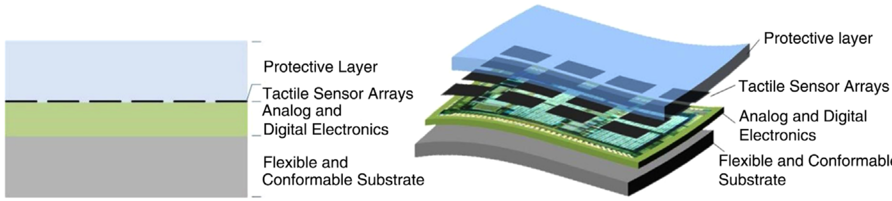

Figure 23.1 General physical structure of the e-skin system.

robustness through redundancy at functional and circuit levels: The drawback is the unavoidable increase of complexity and power consumption.

Next, *sensors* are embedded in a *protective layer*. Sensors can be multimodal in that they can measure different features of the input stimuli, for example, normal and tangential forces. The geometry of the sensor array (i.e., overall area, sensor size, sensor pitch, sensor distribution) depends on the transducer technology and on the given application requirements. The *protective layer*, which is usually polymer based (e.g., PDMS), protects the whole from damages induced by contact with objects, environmental chemical agents and water, and so on. Moreover, it implements a mechanical filtering of the input stimulus and concentrates/distributes the mechanical stimulus onto the sensor array below depending on the thickness and the compliance of the layer. As a consequence, e-skin spatial resolution depends on the sensor geometrical arrangement as well as on the features of this protective layer.

In this chapter, we first study materials and transducers, focusing on most promising sensor technologies. Thereafter, the issue of how to distill useful information from the stream of data produced by tactile sensors is addressed: Raw sensor measurements are processed and organized, trying to infer relations or learning patterns from data collected over time or from different settings. Finally, the tactile information has been interpreted to build a coherent picture of the environment and its evolution over time.

The need of extracting information from multiple sensor data streams impacts on the placement and on the type of sensors, and on the processing throughput and latency. Organizing and fusing sensor data streams so that salient information is extracted is a critical step in the process of sensor data interpretation. The time taken for sensing and interpreting limits the response time in closed-loop control systems. In general, benchmarks and metrics focus on the speed of processing, the quantity of data to be processed, the efficiency of data abstraction, and the associated error rate. As a consequence, efficient real-time embedded implementation is required.

The chapter is organized as follows: Sections 23.1 and 23.2 report a condensed assessment of the state of the art of the available transduction methods and of tactile data processing, respectively. In order to provide an estimation of the computational complexity of the hardware implementation of the processing algorithms, Section 23.3 provides a study of the computational requirements concerning two existing and sound approaches, that is, the electrical impedance tomography (EIT) algorithm [5] and a machine learning (ML) algorithm based on tensorial kernel [6]. Conclusions and future perspectives are reported in Section 23.4.

23.2 The Skin Mechanical Structure

23.2.1 Transducers and Materials

A sensing element can be seen as a structural unit (e.g., capacitive) that produces a signal as a response to a mechanical stimulus or as a material (or aggregation of materials) – for example, piezoelectric [7], piezoresistive [8], and optical [9] – which intrinsically convert the mechanical stress/strain into an optical or electrical signal [10]. When constituted by a mix of different materials having different properties, e-skin shows multimodal sensing capabilities [11], bendability, flexibility, and stretchability, hopefully shrink and wrinkle ability as human skin has [12]. On the basis on what happens in human skin, transduction technologies and corresponding sensors should enable such capabilities as normal and shear force sensing, tensile strain monitoring and vibration detection (at least up to 800 Hz) [13], and e-skin featuring a large frequency bandwidth that spans from 0 to 1 kHz is desirable. According to the application, the spatial resolution (defined as the smallest distance between two distinguishable contact points [14]) should range from a minimum of 1 mm to a maximum of 20–30 mm. Detectable force should span in a range of three orders of magnitude (e.g., 1–1000 g [13]). Even if human skin features high hysteresis, it is preferable that e-skin presents a low hysteresis, to avoid significant processing and complex electronics. The requirements outlined above together with some others (extracted and adapted from literature, in particular from Refs [14–16]) are summarized in Table 23.1. The requirements in Table 23.1 are general and can

Table 23.1 Design requirements for tactile sensing system.

Design criteria		Character guideline
Detectable force range (dynamic range)		0.01–10 N (1000 : 1)
Tactile sensing element (Taxel) pitch (for array only)		≤1 mm for small sensing areas ≥5 mm for large less sensing areas
Spatial resolution		≤1 mm for fingertips 5 mm ÷ 20–30 mm (e.g., limbs, torso, etc.)
Sensor frequency bandwidth (sensor response time)		About 1 kHz (1 ms)
Temporal variation		Both dynamic and static
Mechanical sensing detection capability		Normal and shear forces; vibrations
Sensor system characteristics	Mechanical	Flexible, stretchable, conformable and soft, robust, and durable
	Electrical	Low-power, minimal wiring, and cross talk, electrically and magnetically minimal sensitivity
Sensor response		Monotonic, not necessarily linear, low hysteresis, stable, and repeatable

Source: Adapted from Refs [14–16].

be satisfied totally or partially, according to the target application. Many of the previous requirements are satisfied by many examples reported in the literature, even if, to our knowledge, no e-skin implementation satisfies all of them.

Transduction technologies and the functional materials are the focus of this section. The commonly used are capacitive, piezoelectric, optical, and resistive/piezoresistive (based on conductive polymer films and elastomer composites), with their advantages and disadvantages [13,14,17,18]. Capacitive technology has a well-established design and fabrication technique and it is, along with resistive, the most diffused technology. Capacitive e-skin requires dielectric materials having high dielectric constant (k) to increase sensitivity, and ferroelectric polymers are usually preferred [10]. High-k thin elastomer dielectrics can be developed by an appropriate chemical design, or by addition of high-k fillers or conductive fillers [13] in the elastomer, to design stretchable and flexible capacitive tactile sensors [19,20]. Nanostructured materials like carbon nanotubes (CNT) can enhance sensitivity, dynamic range, and resolution [10]. Capacitive tactile sensors have been developed for small- [21] and large-area tactile sensing [22] and 3D pressure/force sensing [23]. Unfortunately, stray capacitances and cross talk between sensor elements, electromagnetic interference (EMI) sensitivity, and the need of relatively complex electronic circuitry are the most significant drawbacks.

Conductive polymer composite films are used for the development of flexible and compliant large-area resistive-based e-skin, which can be wrapped around curved surfaces. Elastomer composites also are used to realize stretchable resistive sensors [24], although their use is limited to pressure sensing/imaging applications [14] (e.g., electrical impedance tomography by Tawil *et al.* [25]). Stassi *et al.* [17] provides a comprehensive review on the different types of composite materials used in the development of piezoresistive sensing devices. According to Stassi *et al.* [17], e-skin based on resistive solutions and flexible composite materials could give the possibility to satisfy almost all the general requirements presented in Table 23.1. Tactile sensors based on piezoelectric materials – such as PZT, PVDF, PVDF-TrFE, to name but a few – are ideal for dynamic tactile sensing [26] due to their large frequency bandwidth and reduced response time (e.g., useful for monitoring dexterous manipulation, sensing fine surface features and textures). Moreover, piezoelectric materials are mechanically flexible, robust, and present high sensitivity. Examples of small- [27] and large-area [28] piezoelectric-based tactile sensing systems are present in literature. Piezoelectric sensors can exhibit drift in sensor response over time [13] and are mechanically not stretchable. Examples of piezoelectric tactile sensors for 3D force sensing [29,30] exist in literature.

When the number of sensing elements increases, optical-based tactile sensors can be a solution, because of a simplified and cross-talk-free wiring [14] and the possibility to have any electronic component on the sensing areas [31]. Optical tactile sensors can be used for dynamic tactile sensing as well [31]. The use of plastic optical fibers (POFs) allows overcoming sensor limitations related to fragility and rigidity [14]. Polymer-waveguide-based sensors satisfy requirements such as thin film architecture, localized force sensing and multipoint recognition, robustness to bending and fast response times [31], stretchability, stability, low hysteresis and high sensitivity (e.g., weight as low as 10 mg is detectable), and easy to fabricate [32]. For more comprehensive and exhaustive overview of materials and transduction techniques, which is not compatible with the page limits of this chapter, the readers are referred to other recent reviews, for example, Refs [10,13–18,33–35].

In Table 23.2, we report a comparison of the tactile sensing technologies described above and presented in the recent scientific literature (covered years: 2011 to present). In particular, such parameters as hysteresis, bandwidth (or response time), and spatial resolution have not been included as no complete information has been found.

23.2.2 An Example of Skin Integration into an Existing Robotic Platform

While in the next section we will deal with sensor signal processing and interpretation, here we report on how it is possible to practically couple the skin structure to a robotic platform. We illustrate a literature example, consisting in integrating capacitive sensor arrays into the iCub robot.

Effective integration of tactile sensors into real robots requires conformable structures that can be deployed on curved surfaces. Various system-level issues have to be managed, like wiring, networking, power consumption, maintenance, and lowering production costs. Figure 23.2 shows a graphical sketch of the integration of the ROBOSKIN[1] capacitive e-skin system into the iCub robot, as described in Ref. [22]. Similar approaches can be employed for the integration of different skin concepts into other robots.

A skin system for humanoids that integrates distributed pressure sensors based on the capacitive technology has been presented in Ref. [49]. It consists of triangular modules interconnected to form a system of sensors that can be deployed on nonflat surfaces. The basic functional element is a capacitor in which the dielectric deforms when pressure is applied. Patterned conductive areas on a flexible flexible printed circuit board (FPCB) form the first plate of the capacitor. On top of the FPCB, there is a deformable dielectric (3D air mesh fabric) covered by a conductive (Lycra) layer that provides the second plate of the capacitor and works as a common ground plane protecting the sensors from electromagnetic interferences. The third external layer has special hemlines with holes that host screws to keep the cover in place (see Figure 23.3a). Therefore, it can be easily substituted, if damaged, and removed to check the status of the FPCB and electronics below. The FPCB is shaped as a triangle hosting 12 sensors (i.e., taxels) and a capacitance to digital converter (CDC, AD7147 from Analog Devices) performs the AD conversion and transmits the capacitance values to a serial line. Several triangles can be interconnected to form a flexible mesh of sensors to cover the desired area. The triangles and the connections among them are flexible: The resulting mesh can, therefore, be adapted to curved surfaces. The system has been successfully integrated into different humanoid robots, for example, iCub [50],

1 "Skin-Based Technologies and Capabilities for Safe, Autonomous and Interactive Robots" is a FP7 STREP European project.

Table 23.2 Comparison of some tactile sensing technologies reported in international articles and conferences (covered years: 2011–2015).

Reference		Sensitivity		Force/pressure range		$^{(1)}$Bandwidth/ $^{(2)}$Resonant frequency/ $^{(3)}$Cutoff frequency/ $^{(4)}$Sensor response time	Mechanical properties	Linearity	No. of sensors	Sensor size (mm)	$^{(1)}$Repeatability/ $^{(2)}$Stability/ $^{(3)}$Standard deviation
		Normal	Shear	Normal (kPa)	Shear (kPa)						
Capacitive											
2011	[36]	—	1.967fF/N	—	±4 N	<100 Hz	Flexible	Nearly linear	1	3.5 × 1.5 × 5	High$^{(1)}$ 0.428 fF ±2 N range$^{(3)}$ 1.35 fF ±4 N range$^{(3)}$
2012	[37]	0.14 kPa^{-1} 0.05 kPa^{-1}	—	0–5 5–20	—	—	Flexible	Piece-wise linear	4 × 4	3 × 3	—
2013	[23]	0.024 kPa^{-1} 6.6e-4 kPa^{-1}	2.8e-4 kPa^{-1}	0–10 10–140	0–200	10 MHz$^{(3)}$	Flexible	Nearly linear	1 module of 2 × 2 capacitors	0.06 × 4 (each capacitor)	No
2014	[38]	2.24%/MPa	—	240–1000	—	—	Flexible	Almost linear	1	1.5 × 6 × 6	—
2015	[19]	0.001–0.01 kPa^{-1}	–	5–405	–	—	Stretchable	Almost linear	6	9 × 5	Yes$^{(2)}$
Piezoelectric											
2011	[39]	42 mV/N	—	3–5 N	—	—	Flexible	Nearly linear	1	—	Good$^{(1)}$
2013	[40]	0.021 V/mN	–	10–100 mN	–	—	Flexible	Yes	4 × 4	1 mm (radius)	Good$^{(2)}$
2014	[41]	~8 nA/N	—	0.5–8 N	—	—	Flexible	Nearly linear	1	—	Low$^{(1)}$
2015	[42]	430 mV/N (@200 Hz)	—	0.5–2 N	—	Up to 1200 Hz	Flexible	Yes	1	—	—
Resistive/piezoresistive											

2011	[43]	~0.004 kPa^{-1}	—	0–240	—	—	Flexible	Yes	8 × 8	1.5 × 1.5	10% (<150 kPa)$^{(1)}$ 20% (>150 kPa)$^{(1)}$
2012	[44]	—	1.7e-6 Pa^{-1}	—	±1.8	—	Flexible	Yes	1	40 × 40	—
2013	[45]	1.3e−5 kPa^{-1}	1.3e−5 kPa^{-1}	0–400	0–100	—	Flexible	Yes	1	2 × 2 × 0.3	—
2014	[46]	−5.5 kPa^{-1} −0.01 kPa^{-1}	—	<0.1 Pa 0.1–1.4	—	0.2 ms$^{(4)}$	Flexible	—	1 (graphene array)	2 cm^2	Good$^{(1)}$ Good$^{(2)}$
2015	[8]	−0.5 kPa^{-1}	—	~0–30	—	—	Flexible	—	8 × 8	1 × 1	High$^{(1)}$
Optical											
2011	[9]	−26,7 (ΔV/mV)/g	—	0–40 g	—	600 ms$^{(4)}$	Flexible	Almost	1	30 × 30	High$^{(2)}$
2012	[32]	0.02 kPa^{-1} 0.025 kPa^{-1}(when stretched) 0.05 kPa^{-1} (when bent)	—	0–5 10 (const load) 10 (const load)	—	300 ms$^{(4)}$	Stretchable	No	1	50 × 50	Good$^{(2)}$
2013	[47]	0.8 pm/Pa	1.3 pm/Pa	<2.4 kPa	≤0.6	—	Soft	Almost	1	27 × 27 × 22	No
2014	[48]	~0.1 V/N	~0.1 V/N	0–8 N	0–2 N	1 ms$^{(4)}$	Stretchability if stretchable wiring	Yes	6 × 6 (each sensor has 2 × 2 taxels)	6.4 × 6.4	6.77% (error)$^{(1)}$

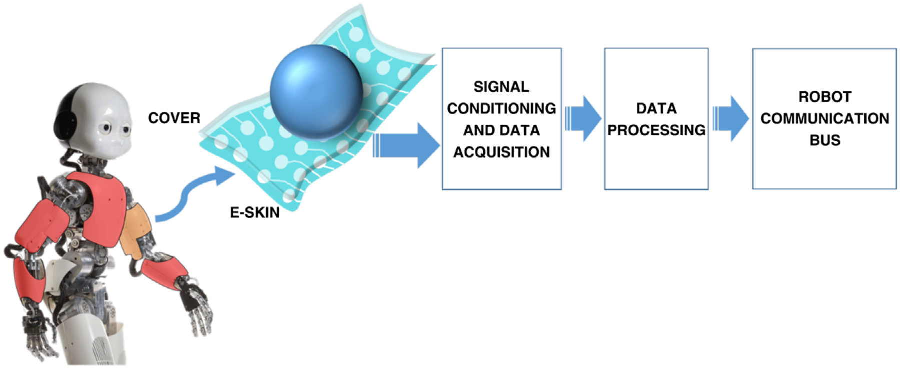

Figure 23.2 Graphical sketch of the integration of the ROBOSKIN e-skin system into iCub. (Image courtesy of the Italian Institute of Technology – IIT, Genova, Italy).

KASPAR [51], and NAO [52], and also the Schunk robotic arm as shown in Figure 23.4.

The following are the steps that were pursued for the skin integration into the iCub forearm:

- The mesh of triangles (see Figure 23.4) was glued on the cover of the iCub forearm using a bicomponent glue and with the help of a vacuum system in order to improve the adhesion on the 3D surface. In Figure 23.3c, it is possible to see the final result of this procedure.
- For the dielectric layer, different layers of fabric have been glued together, cut, and shaped to adapt to the robot part. The cover was then mounted and fixed with screws to the iCub forearm (see Figure 23.3a and b): This allows easy mounting and substitution. This procedure has been pursued for the integration of the sensor arrays on other iCub parts (the two arms, palms and torso, and also on the WAM arm from Barret Technology [22]).

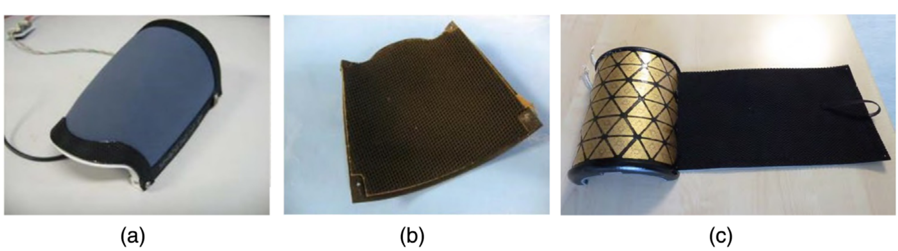

Figure 23.3 The sole dielectric layer that has been integrated into the sensor array in this version of the capacitive skin. (a) Front side. (b) Back side. (c) The complete skin patch (dielectric layer unrolled on the side) as mounted on the Schunk robotic arm. (Image courtesy of the Italian Institute of Technology – IIT, Genova, Italy).

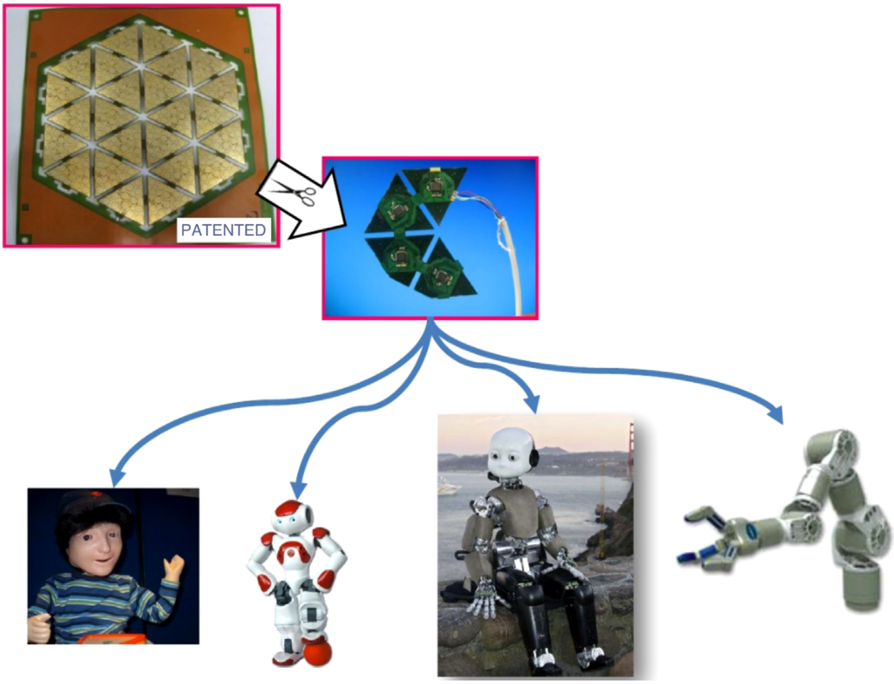

Figure 23.4 Capacitive e-skin applied to different robots. (Image courtesy of the Italian Institute of Technology – IIT, Genova, Italy).

23.3 Tactile Information Processing

Approaching tactile sensing at a *system* level means managing all issues associated with the integration of data processing and information management into a sensitive system built on structural and functional host materials. In this chapter, we limit the overview to what information is relevant and which are available methods to extract it from sensor data, discarding the wider problem of interpreting and reacting on the basis of this available structured and unstructured tactile information.

What kind of information is being propagated from the sensitized object to the robot/human? Interesting information about the minimum functional requirements for a robotic tactile sensing system mimicking human in-hand *manipulation* is contained in Ref. [14]. Those requirements shed light on what is needed to be detected during tactile contact for the complex manipulation process. An interesting review is contained in Ref. [53], in that HRI (human–robot interaction) context with the scope of summarizing (i) what is detected during tactile contact of a robot with a human and (ii) how the detected information is used by the robot. As said above, we only focus on aspect (i). Without pretending to be exhaustive, Table 23.3 extends what is reported in Ref. [53], including relevant references from journal publications only, published during 2005–2015.

Table 23.3 What information is extracted from sensor data (covered years: 2005–2015, journal publications only).

Contact	Location	[5,22,54–60]
	Area	[5,28,56,60–66]
	Static	[22,23,40,61–63,65,67–70]
	Dynamic	[28,30,43,45,54,64,69,71–73]
Force	Normal	[5,22,23,45,56–58,66,67,72,74–78]
	Shear	[23,40,45,67,68,74–77]
	Magnitude (intensity)	[23,45,56–60,66,67,70,72]
	Orientation (direction)	[23,40,45,59,60,67,70,72,74–76]
	Moment	[72,79–81]
	Pressure distribution (only normal force)	[22,24,32,54,63–65,82–84]
	Whole force distribution	[61,62,85,86]
High-Level Info	Texture/roughness	[71,87–94]
	Stiffness (contact object)	[24,54]
	Slip detection	[18,30,71,95–98]
	Vibration	[71,72]
	Touch modality	[5,6,66,99–103]

Tactile data processing concerns *lower level* information as that required for object grasping and manipulation and related to an accurate estimation of finger–object interaction such as contact location, area and duration, contact force intensity, direction and distribution, together with temperature. Touch also enables more *high-level* information for the classification of attributes of the contacting objects, for example, roughness, textures, patterns, shapes, as well as data related to object movement on the cutaneous surface, for example, slip detection, vibration, up to the discrimination of the touch modality.

Except for temperature, which is still a hot topic, which deserves a specific discussion, and which is beyond the scope of the present study, what is named *low-level* information can be faced either using *distributed* or *concentrated* approach.

In a distributed approach, complete information is attributable to the reconstruction of the force distribution at a given instant [48,104]. Either regularization methods (e.g., Tichonov) have been used in specific systems to deal with the ill-posed problem of retrieving the (continuum) complete force distribution starting from (finite) sensor data [105] or case-by-case approaches are used and specific sensor arrangements have been proposed leading to three-axis contact force distribution [61,62,85]. On the other hand, a general method for the reconstruction of the spatial distribution of contact forces as well as their intensities and directions starting from embedded sensor data has been recently proposed [86]. In this case, continuum mechanics is used as a framework for the direct problem of mechanical stimuli transmission to the sensor array and the problem is inverted using an optimization procedure and accounting for the physics of the problem. The importance of this method resides in its generality, as it is independent of the specific employed transducer and tactile application, provided that stress information comes from embedded sensor in an elastic layer.

More frequently, the distribution of the sole normal component of the force (pressure) is reconstructed, which allows for punctual information that is however far from being complete [22,24,32,54,63–65,82–84].

In a concentrated approach, either force resultants and moments are available and the contact location (centroid position at each instant) can be retrieved [79] or contact location(s), the force resultant(s), and point(s) of application are known and moments can be calculated [80].

While treating object movement on the cutaneous surface, dynamic sensors are involved (see Table 23.3). In this context, sliding systems have to be cited as they are relevant from the point of view of applications. For interesting literature about sliding and slip prevention, whose in-depth analysis is not at the core of this discussion, the reader is referred to Refs [18,30,95,96] and references therein.

Slip detection can be either inferred directly from vibration signals [30,71,106–108] or indirectly by characterizing and identifying the dynamic force variations associated with slip [97,98]. A widespread method (also used in prosthetic commercial systems[2]) to avoid sliding is to monitor the normal and shear force from a grasped object [23,45,67,74–77], while keeping the normal-to-tangential force ratio above a certain value [109]. Measurement of 3D contact forces is also critical for determining the full grasp force/torque and for handling fragile and irregular objects.

Other topics that are related to moving touches are the discrimination of textures and the interpretation of touch modalities [99], although in the context of social robotics information other than tactile (e.g., vision) probably needs to be involved – like for humans – to properly discriminate the modality of touch. To deepen these concepts, the reader is referred to Ref. [100] and references therein. If the tactile-sensing framework has to face such challenging assignments such as texture and touch modality recognition, machine learning techniques [110] may prove to be useful as explicit formalization of the input–output relationship is difficult to attain. In this case, the actual problem is to discriminate between a set of stimuli that the system is expected to recognize and empirical induction is used by learning-from-examples approach. Machine learning paradigms represent a powerful technology for tackling clustering, classification, and regression problems in complex domains and they have been widely used in robotics to retrieve partial contact information on specific systems [66,87–89,100,111]. Nevertheless, ML has its own limitations and the quality of results depends on the quality of training data and also generality is not warranted.

All these processing aspects can be integrated into overall systems that closely resembles to the human skin. Very interesting examples are reported in a recent review [13], which includes all existing research on multimodal systems that retrieve both structured and unstructured tactile information. To cite an example,

2 www.ottobock.com.

multimodal HEX-O-SKIN [1,71] measures normal and shear forces together with the hardness of the contact object and vibrations, enabling slip detection, impact sensation, and contact roughness sensing.

23.4 Computational Requirements

Besides the huge amount of tactile data to be processed in real time, the computation complexity poses a tough challenge in the development of the embedded electronic system. Computational requirements depend on the overall number of operations (mainly arithmetic) that the algorithm must perform and on the real-time operation.

This section presents an assessment of the computational requirements taking into account two sound and completed approaches: (i) electrical impedance tomography to classify social touch [5]; (ii) tensorial kernel approach to classify touch modality [101]. Figure 23.5 shows the algorithmic steps needed to classify the input touch: In the EIT approach, the complexity of the computation mainly lies in the first step (EIT inverse solution); while in the tensorial kernel approach, it lies in the singular value decomposition.

23.4.1 Electrical Impedance Tomography

Electrical impedance tomography is an imaging technique used to estimate the internal conductivity distribution of an electrically conductive body based on

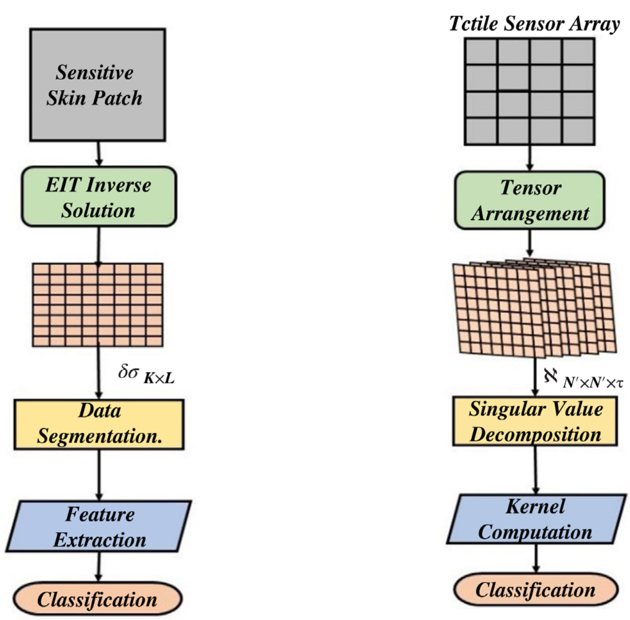

(a) (b)

Figure 23.5 Algorithmic steps: (a) EIT and (b) tensorial kernel approaches.

electrical (i.e., voltages and/or currents) measurements made only at the boundary. In tactile systems, a conductive patch is used as sensitive skin; when a contact on the sensitive skin happens, the conductivity distribution changes as a consequence and the EIT reconstruction problem consists in finding the distribution of conductivity due to the contact; the result is an image displaying the distribution of conductivity and consequently the contact force/pression distribution. The EIT reconstruction problem is a nonlinear inverse problem where a unique solution does not exist (ill-conditioned problem). The starting point for EIT is Maxwell's equations for electromagnetics. A commonly used approach to solve the mathematical model represented by the Maxwell differential equations is the finite element method (FEM) [112]. At each iteration, the multiplication of a sparse $M \times M$ matrix by $1 \times M$ vector (where M is the number of potential measurements on the boundary) is implemented. In Ref. [5], the ill-conditioned problem has been solved by using the generalized Tikhonov regularization [113–115]. The solution figures out a matrix $\delta\sigma_{K \times L}$ containing the difference between the conductivity of the input contact and a conductivity σ_0 taken as reference. K is the number of elements in the FEM mesh and L is the number of injection current patterns [25].

The classification of touch modalities is done using "LogitBoost" classifier. Table 23.4 shows the operations needed to implement the EIT method.

23.4.2 Tensorial Kernel

Machine learning approaches have not been developed to handle data that are represented in the form of tensors, that is, n-dimension input vectors; hence, the implementation of some feature extraction process is needed to map tensor signals into multidimensional vectors, with the risk of compromising the original structural and topological information [116,117]. The ML-based approach in Ref. [101] proposes a tensor-based morphology of tactile signals, in a marked analogy with image tensor constructed from face images for face recognition application [36].

Tensorial kernel approach consists of first computing the singular value decomposition (SVD) [37] of the input tactile $N' \times N'$ matrix. The study of the computational requirements for the SVD is based on the *one-sided Jacobi*

Table 23.4 The computational requirements [5]; N_t is the number of training data.

Operation	FEM	Tikhonov regularization	Classification
Addition/ subtraction	$M^2(M-1)+\frac{M}{6}(20M^2 -3M-5)$	$\frac{K}{6}(20K^2-5+6KM-3K) +KM(L+K-1)-KL$	$M \times (2M+3) \times 3N_t$
Multiplication	M^3	$KM\ (2K+L)$	$M \times (M+6) \times 3N_t$
Division	0	MK	$2 \times M \times 3N_t$
Square root	0	K^2	0

Table 23.5 The computational requirements [101]; N is the dimension of the matrix, K^* is the number of SVD iterations, and N_{sv} is the number of support vectors.

Operation	SVD	Kernel function	Classification
Addition/subtraction	$\frac{3}{2}N'(N'-1)\left[2N'^2(N'-1)+4\right]K^*$	$3N'(2N'^2-1)$	$(1+3Nt)\times N_{sv}$
Multiplication	$\frac{3}{2}N'(N'-1)(2N'^3+3)K^*$	$3N'^2(2N'+1)+5$	$3Nt\times N_{sv}$
Division	$\frac{9}{2}N'(N'-1)K^*$	0	0
Square-root	$3N'(N'-1)K^*$	0	0

algorithm that provides high accuracy and convergence in about $K^*=5$–10 iterations [38]. Following step is the computation of the kernel function for a couple of SVDs, the first corresponds to the tensor input and the second to the tensor representing a predefined class extracted from the training data. Table 23.5 shows the operations needed to implement the tensorial kernel approach.

In order to assess the computational burden, a case study with the setups used in Refs [5,101] has been considered. The task is to classify an input touch with duration of $\tau = 1$ s into three touch modalities; the number of training data is set to $N_t = 100$. In Ref. [5], a total of $M = 224$ V measurements were needed at each acquisition step. A total of $K = 2240$ elements in the FEM mesh were used for the forward solution. The number of iterations of the LogitBoost classifier needed to converge is $M' = 25$. In Ref. [101], the input matrix has size 8×8 sensors; for the duration of touch $\tau = 1$ s, three different matrix sizes ($N' = 8$, $N' = 8$, and $N' = 64$) have to be decomposed by the SVD. The number of SVD iterations using the one-sided Jacobi algorithm is $K^* = 8$; the number of support vectors has been set to $N_{sv} = 50$. Table 23.6 shows the results of the case study in terms of number of operations.

Following Table 23.6 results, about 42 Giga-operations/s [5] and about 31 Giga-operations/s [101] are needed for a real-time single-touch classification (three classes). The requirements for the processing unit are very challenging; for instance, let us consider the very well-known ARM Cortex processor family [39]. The ARM Cortex-R are high-performance processors, meeting challenging real-time constraints: they offer high-performance computing solutions for real-time

Table 23.6 Number of operations needed for a single-input touch classification [5,101].

Operation	EIT	Tensorial kernel
Addition/subtraction	3.97×10^{10}	1.56×10^{10}
Multiplication	2.28×10^{9}	1.58×10^{10}
Division	6.36×10^{5}	6.48×10^{5}
Square root	5.01×10^{6}	4.32×10^{5}

embedded systems. The Cortex-R7 processor architecture reduces latency and enables symmetric multiprocessing in a dual-core configuration. Cortex-R7 can achieve 3 GIPS/core: The dual-core architecture is not able to achieve the target requirements as highlighted in Table 23.6.

One possible approach to tackle this issue could be to design a multiprocessor Cortex-R7 architecture on FPGA. Alternative solution is to design a dedicated ASIC either on FPGA or on a standard cell technology; although this solution is expensive, it allows the optimization of the parallel implementation and to fulfill target requirements.

23.5 Conclusions

The chapter reviews and assesses current trends in the development of an electronic skin. We addressed such an issue from a system perspective, starting from basic building components (materials, electronics) and approaching toward the complete skin system, taking into the due course embedded tactile data processing. We first focused our discussion and literature review on capacitive, piezoelectric, optical, and resistive/piezoresistive sensors, which are well-established and most relevant and promising tactile transduction techniques. As a next step, while the most demanding applications require capabilities of both perceiving the environment, interpreting it, and of basing decisions and actions on perception, we focused on the step before, consisting in analyzing data processing methods that provide useful tactile information while leaving the human brain the responsibility of deciding on how to proceed.

The embedded electronic system raises a number of issues: It must be compliant with the e-skin structure, that is, flexible, it must consume low power (heat dissipation is another cumbersome issue to be tackled), it must be implemented in the real-time complex processing tasks with a huge amount of tactile data to manage, it must be robust against electrical noise and mechanical damages, and must be resilient. All such demanding requirements are very difficult to achieve with currently available approaches; relevant research and engineering efforts must be devoted to this scope.

References

1 Mittendorfer, P. and Cheng, G. (2012) Integrating discrete force cells into multi-modal artificial skin. 12th IEEE-RAS International Conference on Humanoid Robots, Nov. 29–Dec. 1, Business Innovation Center Osaka, Japan.

2 Bossuyt, F., Vervust, T., and Vanfleteren, J. (2013) Stretchable electronics technology for large area applications: fabrication and mechanical characterization. *IEEE Transactions on Components, Packaging and Manufacturing Technology*, **3** (2), 229–235.

3 van den Brand, J., de Kok, M., Sridhar, A., Cauwe, M., Verplancke, R., Bossuyt, F., de Baets, J., and Vanfleteren, J. (2014) Flexible and stretchable electronics for wearable healthcare. The 44th European Solid State Device

Research Conference (ESSDERC), pp. 206–209. doi: 10.1109/ESSDERC.2014.6948796

4 Rogers, J.A., Someya, T., and Huang, Y. (2010) Materials and mechanics for stretchable electronics. *Science*, **327** (5973), 1603–1607.

5 Silvera Tawil, D., Rye, D., and Velonaki, M. (2014) Interpretation of social touch on an artificial arm covered with an EIT-based sensitive skin. *Journal of Social Robotics*, **6** (4), 489–505.

6 Gastaldo, P., Pinna, L., Seminara, L., Valle, M., and Zunino, R. (2015) A tensor-based approach to touch modality classification by using machine learning. *Robotics and Autonomous Systems*, **63**, 268–278.

7 Ramadan, K.S., Sameoto, D., and Evoy, S. (2014) A review of piezoelectric polymers as functional materials for electromechanical transducers. *Smart Materials and Structures*, **23** (3), 033001.

8 Ma, C.-W., Lin, T.-H., and Yang, Y.-J. (2015) Tunneling piezoresistive tactile sensing array fabricated by a novel fabrication process with membrane filters. 28th IEEE International Conference on Micro Electro Mechanical Systems (MEMS), Jan. 18–22, 2015, pp. 249–252. doi: 10.1109/MEMSYS.2015.7050935

9 Massaro, A., Spano, F., Lay-Ekuakille, A., Cazzato, P., Cingolani, R., and Athanassiou, A. (2011) Design and characterization of a nanocomposite pressure sensor implemented in a tactile robotic system, instrumentation and measurement. *IEEE Transactions on Instrumentation and Measurement*, **60** (8), 2967–2975.

10 Saraf, R. and Maheshwari, V. (2008) Tactile devices to sense touch on a par with a human finger. *Angewandte Chemie, International Edition*, **47**, 7808–7826.

11 Kim, J., Lee, M., Shim, H.J., Ghaffari, R., Cho, H.R., Son, D., Jung, Y.H., Soh, M., Choi, C., Jung, S., Chu, K., Jeon, D., Lee, S.-T., Kim, J.H., Choi, S.H., Hyeon, T., and Kim, D.-H. (2014) Stretchable silicon nanoribbon electronics for skin prosthesis. *Nature Communications*, **5** (5747). doi: 10.1038/ncomms6747

12 Lumelsky, V.J., Shur, M.S., and Wagner, S. (2001) Sensitive skin. *IEEE Sensors Journal*, **1** (1). doi: 10.1109/JSEN.2001.923586

13 Hammock, M.L., Chortos, A., Tee, B.C.-K., Tok, J.B.-H., and Bao, Z. (2013) 25th anniversary article: the evolution of electronic skin (e-skin): a brief history, design considerations, and recent progress. *Advanced Materials*, **25**, 5997–6038.

14 Yousef, H., Boukallel, M., and Althoefer, K. (2011) Tactile sensing for dexterous in-hand manipulation in robotics: a review. *Sensors and Actuators A*, **167**, 171–187.

15 Mehrizi, A., Dargahi, J., and Najarian, S. (2009) *Artificial Tactile Sensing in Biomedical Engineering*, McGraw-Hill.

16 Dahiya, R.S., Metta, G., Valle, M., and Sandini, G. (2010) Tactile sensing: from humans to humanoids. *IEEE Transactions on Robotics*, **26** (1), 1–20.

17 Stassi, S., Cauda, V., Canavese, G., and Fabrizio Pirri, C. (2014) Flexible tactile sensing based on piezoresistive composites: a review. *Sensors*, **14** (3), 5296–5332.

18 Tiwana, M.I., Redmond, S.J., and Lovell, N.H. (2012) A review of tactile sensing technologies with applications in biomedical engineering. *Sensors and Actuators A*, **179**, 17–31.

19 Gerratt, A.P., Michaud, H.O., and Lacour, S.P. (2015) Elastomeric electronic skin for prosthetic tactile sensation. *Advanced Functional Materials*, **25** (15), 2287–2295.

20 Park, S., Kim, H., Vosgueritchian, M., Cheon, S., Kim, H., Koo, J.H., Kim, T.R., Lee, S., Schwartz, G., Chang, H., and Bao, Z. (2014) Stretchable energy-harvesting tactile electronic skin capable of differentiating multiple mechanical stimuli modes. *Advanced Materials*, **26**, 7324–7332.

21 Tsai, T.-H., Tsai, H.-C., and Wu, T.-K. (2014) A CMOS micromachined capacitive tactile sensor with integrated readout circuits and compensation of process variations. *IEEE Transactions on Biomedical Circuits and Systems*, (99), 1–9.

22 Maiolino, P., Maggiali, M., Cannata, G., Metta, G., and Natale, L. (2013) A flexible and robust large scale capacitive tactile system for robots. *IEEE Sensors Journal*, **13** (10), 3910–3917.

23 Dobrzynska, J.A. and Gijs, M.A.M. (2020) Polymer-based flexible capacitive sensor for three-axial force measurements. *Journal of Micromechanics and Microengineering*, **23** (1), 015009

24 Cheng, M.-Y., Tsao, C.-M., Lai, Y.-Z., and Yang, Y.-J. (2011) The development of a highly twistable tactile sensing array with stretchable helical electrodes. *Sensors and Actuators A*, **166** (2), 226–233.

25 Tawil, D.S., Rye, D., and Velonaki, M. (2011) Improved image reconstruction for an EIT-based sensitive skin with multiple internal electrodes. *IEEE Transactions on Robotics*, **27** (3), 425–435.

26 Howe, R.D. and Cutkosky, M.R. (1993) Dynamic tactile sensing: perception of fine surface features with stress rate sensing. *IEEE Transactions on Robotics and Automation*, **9** (2), 140–151.

27 Dahiya, R.S., Adami, A., Pinna, L., Collini, C., Valle, M., and Lorenzelli, L. (2014) Tactile sensing chips with POSFET array and integrated interface electronics. *IEEE Sensors Journal*, **14** (10), 3448–3457.

28 Seminara, L., Pinna, L., Valle, L.M., Basirico, L., Loi, A., Cosseddu, P., Bonfiglio, A., Ascia, A., Biso, M., Ansaldo, A., Ricci, D., and Metta, G. (2013) Piezoelectric polymer transducer arrays for flexible tactile sensors. *IEEE Sensors Journal*, **13** (10), 4022–4029.

29 Faramarzi, S., Ghanbari, A., Chen, X.Q., and Wang, W.H. (2009) A PVDF based 3D force sensor for micro and nano manipulation IEEE International Conference on Control and Automation (ICCA'09), Dec. 9–11, 2009. pp. 867–871. doi: 10.1109/ICCA.2009.5410237

30 Cotton, D.P.J., Chappell, P.H., Cranny, A., White, N.M., and Beeby, S.P. (2007) A novel thick-film piezoelectric slip sensor for a prosthetic hand. *IEEE Sensors Journal*, **7** (5), 752–761.

31 Yun, S., Park, S., Park, B., Kim, Y., Park, S.K., Nam, S., and Kyung, K.-U. (2014) Polymer-waveguide-based flexible tactile sensor array for dynamic response. *Advanced Materials*, **26**, 4474–4480.

32 Ramuz, M., Tee, B.C.-K., Tok, J.B.-H., and Bao, Z. (2012) Transparent, optical, pressure-sensitive artificial skin for large-area stretchable electronics. *Advanced Materials*, **24**, 3223–3227.

33 Dahiya, R.S., Mittenderfer, P., Valle, M., Cheng, G., and Lumelsky, V.J. (2013) Directions toward effective utilization of tactile skin: a review. *IEEE Sensors Journal*, **13** (11), 4121–4138.

34 Chortos, A. and Bao, Z. (2014) Skin-inspired electronic devices. *Materials Today*, **17** (7), 321–331.

35 Sokhanvar, S., Dargahi, J., Najarian, S., and Arbatani, S. (2012) Tactile sensing technologies, in *Tactile Sensing and Displays: Haptic Feedback for Minimally Invasive Surgery and Robotics*, John Wiley & Sons, Ltd, Chichester, UK.

36 Jinseok, L. and Daijin, K. (2009) Tensor-based AAM with continuous variation estimation: application to variation-robust face recognition. *IEEE Transactions on Pattern Analysis and Machine Intelligence*, **31** (6), 1102–1116.

37 Ledesma-Carrillo, L.M., Cabal-Yepez, E., Romero-Troncoso, R.de J., Garcia-Perez, A., Osornio-Rios, R.A., and Carozzi, T.D. (2011) Reconfigurable FPGA based unit for singular value decomposition of large $m \times n$ matrices. International Conference on Reconfigurable Computing and FPGAs.

38 Wang, X. and Zambreno., J. (2014) An FPGA implementation of the Hestenes–Jacobi algorithm for singular value decomposition. IEEE 28th International Parallel & Distributed Processing Symposium Workshops.

39 infocenter.arm.com/help/index.jsp?topic=/com.arm.doc.set.cortexr/index.html.

40 Tiwana, M.I., Shashank, A., Redmond, S.J., and Lovell, N.H. (2011) Characterization of a capacitive tactile shear sensor for application in robotic and upper limb prostheses. *Sensors and Actuators A*, **165** (2), 164–172.

41 Chen, C.-C., Chang, P.-Z., and Shih, W.-P. (2012) Flexible tactile sensor with high sensitivity utilizing botanical epidermal cell natural micro-structures. *IEEE Sensors Journal*, 1–4.

42 Lei, K.F., Lee, K.-F., and Lee, M.-Y. (2014) A flexible PDMS capacitive tactile sensor with adjustable measurement range for plantar pressure measurement. *Microsystem Technologies*, **20** (7), 1351–1358.

43 Wang, Y.R., Zheng, J.M., Ren, G.Y., Zhang, P.H., and Xu, C. (2011) A flexible piezoelectric force sensor based on PVDF fabrics. *Smart Materials and Structures*, **20** (4), 045009.

44 Kim, M.S., Jo, S.E., Kang, D.H., Ahn, H.R., and Kim, Y.J. (2013) A dome shaped piezoelectric tactile sensor array using controlled inflation technique. The 17th International Conference on Solid-State Sensors, Actuators and Microsystems (Transducers & Eurosensors XXVII), June 16–20, 2013, pp. 1891–1894. doi: 10.1109/Transducers.2013.6627161

45 Beccai, L., Roccella, S., Ascari, L., Valdastri, P., Sieber, A., Carrozza, M., and Dario, P. (2008) Development and experimental analysis of a soft compliant tactile microsensor for anthropomorphic artificial hand. *IEEE/ASME Transactions on Mechatronics*, **13**, 158–168.

46 Cosseddu, P., Viola, F., Lai, S., Raffo, L., Seminara, L., Pinna, L., Valle, M., Dahiya, R., and Bonfiglio, A. (2014) Tactile sensors with integrated piezoelectric polymer and low voltage organic thin-film transistors. *IEEE Sensors Journal*, pp. 1734–1736. doi: 10.1109/ICSENS.2014.6985358

47 Maita, F., Maiolo, L., Minotti, A., Pecora, A., Ricci, D., Metta, G., Scandurra, G., Giusi, G., Ciofi, C., and Fortunato, G. (2015) Ultra-flexible tactile piezoelectric

sensor based on low-temperature polycrystalline silicon thin film transistor technology. *IEEE Sensors Journal*. doi: 10.1109/JSEN.2015.2399531.
48 Fearing, R.S. (1990) Tactile sensing mechanisms. *International Journal of Robotics Research*, **9** (3), 3–23.
49 Schmitz, A., Maiolino, P., Maggiali, M., Natale, L., Cannata, G., and Metta, G. (2011) Methods and technologies for the implementation of large-scale robot tactile sensors. *IEEE Transactions on Robotics*, **27** (3), 389–400.
50 Metta, G., Vernon, D., Natale, L., Nori, F., and Sandini, G. (2008) The iCub humanoid robot: an open platform for research in embodied cognition. Presented at IEEE Workshop on Performance Metrics Intelligent Systems, San Jose, CA.
51 Dautenhahn, K., Nehaniva, C.L., Waltersa, M.L., Robins, B., Kose-Bagcia, H., Mirzaa, N.A., and Blow, M. (2009) KASPAR: a minimally expressive humanoid robot for human–robot interaction research. *Applied Bionics and Biomechanics*, **6** (3), 369–397.
52 Dahl, T.S. and Palmer, A. (2010) Touch-triggered protective reflexes for safer robots. Proceedings of the International Symposium on New Frontiers in Human–Robot Interactions, p. 7.
53 Argall, B.D. and Billard, A.G. (2010) A survey of tactile human–robot interactions. *Robotics and Autonomous Systems*, **58**, 1159–1176.
54 Sokhanvar, S., Packrisamy, M., and Dargahi, J. (2007) A multifunctional PVDF-based tactile sensor for minimally invasive surgery. *Smart Materials and Structures*, **16**, 989–998.
55 Aucouturier, J.-J., Ikeuchi, K., Hirukawa, H., Nakaoka, S., Shiratori, T., Kudoh, S., Kanehiro, F., Ogata, T., Kozima, H., Okuno, H.G., Michalowski, M.P., Ogai, Y., Ikegami, T., Kosuge, K., Takeda, T., and Hirata, Y. (2008) Cheek to chip: dancing robots and AI's future. *IEEE Intelligent Systems*, **23** (2), 1541–1672.
56 Miyashita, T., Tajika, T., Ishiguro, H., Kogure, K., and Hagita, N. (2007) Haptic communication between humans and robots, in *Robotics Research*, vol. 28, Springer, Berlin, Germany, pp. 525–536.
57 Mukai, T., Onishi, M., Odashima, T., Hirano, S., and Luo, Z. (2008) Development of the tactile sensor system of a human-interactive robot RI-MAN. *IEEE Transactions on Robotics*, **24** (2), 505–512.
58 Nishio, S., Ishiguro, H., and Hagita, N. (2007) Geminoid: teleoperated android of an existing person, in *Humanoid Robots: New Developments* (ed. A.C. de Pina Filho), I-Tech, Vienna, Austria.
59 Wettels, N., Santos, V., Johansson, R., and Loeb, G. (2008) Biomimetic tactile sensor array. *Advanced Robotics*, **22**, 829–849.
60 Yamada, Y., Morizono, T., Umetani, Y., and Takahashi, H. (2005) Highly soft viscoelastic robot skin with a contact object-location-sensing capability. *IEEE Transactions on Industrial Electronics*, **52** (4), 960–968.
61 Lee, H.-K., Chung, J., Chang, S.-I., and Yoon, E. (2008) Normal and shear force measurement using a flexible polymer tactile sensor with embedded multiple capacitors. *Journal of Microelectromechanical Systems*, **17** (4), 934–942.
62 Lee, H.K., Chung, J., Chang, S.I., and Yoon, E. (2011) Real-time measurement of the three-axis contact force distribution using a flexible capacitive polymer tactile sensor. *Journal of Micromechanics and Microengineering*, **21** (3), 035010.

63 Barbaro, M., Caboni, A., Cosseddu, P., Mattana, G., and Bonfiglio, A. (2010) Active devices based on organic semiconductors for wearable applications. *IEEE Transactions on Information Technology in Biomedicine*, **14** (3), 758–766.
64 Dahiya, R.S., Adami, A., Collini, C., and Lorenzelli, L. (2013) POSFET tactile sensing arrays using CMOS technology. *Sensors and Actuators A*, **202**, 226–232.
65 Mannsfeld, S.C.B., Tee, B.C., Stoltenberg, R.M., Chen, C.V.H., Barman, S., Muir, B.V.O., Sokolov, A.N., Reese, C., and Bao, Z. (2010) Highly sensitive flexible pressure sensors with microstructured rubber dielectric layers. *Nature Materials*, **9** (10), 859–864.
66 Iwata, H. and Sugano, S. (2005) Human–robot-contact-state identification based on tactile recognition. *IEEE Transactions on Industrial Electronics*, **52** (6), 1468–1477.
67 Takahashi, H., Nakai, A., Thanh-Vinh, N., Matsumoto, K., and Shimoyama, I. (2013) A triaxial tactile sensor without crosstalk using pairs of piezoresistive beams with sidewall doping. *Sensors and Actuators A*, **199**, 43–48.
68 Noda, K., Onoe, H., Iwase, E., Matsumoto, K., and Shimoyama, I. (2012) Flexible tactile sensor for shear stress measurement using transferred sub-μm-thick Si piezoresistive cantilevers. *Journal of Micromechanics and Microengineering*, **22** (11). doi: 10.1088/0960-1317/22/11/115025
69 Dargahi, J., Rao, N., and Sokhanvar, S. (2006) Design and microfabrication of a hybrid piezoelectric-capacitive tactile sensor. *Sensor Review*, **26** (3), 186–192.
70 da Rocha, J.G.V. and Lanceros-Mendez, S. (2009) Capacitive sensor for three-axis force measurements and its readout electronics. *IEEE Transactions on Instrumentation and Measurement*, **58**, 2830–2836.
71 Mittendorfer, P. and Cheng, G. (2011) Humanoid multimodal tactile-sensing modules. *IEEE Transaction on Robotics*, **27** (3), 401–410.
72 Schmidt, P.A., Maël, E., and Würtz, R.P. (2006) A sensor for dynamic tactile information with applications in human–robot interaction and object exploration. *Robotics and Autonomous Systems*, **54** (12), 1005–1014.
73 Qasaimeh, M., Sokhanvar, S., Dargahi, J., and Kahrizi, M. (2009) PVDF-based microfabricated tactile sensor for minimally invasive surgery. *Journal of Microelectromechanical Systems*, **18** (1), 195–207.
74 Choi, W.-C. (2010) Polymer micromachined flexible tactile sensor for three-axial loads detection. *Transactions on Electrical and Electronic Materials*, **11** (3), 130–133.
75 Huang, Y., Sohgawa, M., Yamashita, K., Kanashima, T., Okuyama, M., Noda, M., and Noma, H. (2008) Fabrication and normal/shear stress responses of tactile sensors of polymer/Si cantilevers embedded in PDMS and urethane gel elastomers. *IEEE Transactions on Sensors and Micromachines*, **128**, 193–197.
76 Kim, K., Lee, K.R., Lee, D.S., Cho, N.-K., Kim, W.H., Park, K.-B., Park, H.-D., Kim, Y.K., Park, Y.-K., and Kim, J.-H. (2006) A silicon-based flexible tactile sensor for ubiquitous robot companion applications. *Journal of Physics*, **34**, 399–403.
77 Valdastri, P., Roccella, S., Beccai, L., Cattin, E., Menciassi, A., Carrozza, M.C., and Dario, P. (2005) Characterization of a novel hybrid silicon three-axial force sensor. *Sensors and Actuators A*, **123–124**, 249–257.

78 Yussof, H., Ohka, M., Kobayashi, H., Takata, J., Yamano, M., and Nasu, Y. (2007) Development of an optical three-axis tactile sensor for object handing tasks in humanoid robot navigation system. *Studies in Computational Intelligence*, **76**, 43–51.

79 Liu, H., Nguyen, K.C., Perdereau, V., Bimbo, J., Back, J., Godden, M., Seneviratne, L.D., and Althoefer, K. (2015) Finger contact sensing and the application in dexterous hand manipulation. *Autonomous Robots*, **39** (1), 25–41.

80 Fumagalli, M., Ivaldi, S., Randazzo, M., Natale, L., Metta, G., Sandini, G., and Nori, F. (2012) Force feedback exploiting tactile and proximal force/torque sensing. *Autonomous Robots*, **33**, 381–398.

81 De Maria, G., Natale, C., and Pirozzi, S. (2012) Force/tactile sensor for robotic applications. *Sensors and Actuators. A*, **175**, 60–72.

82 Kawaguchi, H., Someya, T., Sekitani, T., and Sakurai, T. (2005) Cut-and-paste customization of organic FET integrated circuit and its application to electronic artificial skin. *IEEE Journal of Solid-State Circuits*, **40** (1), 177–185.

83 Yang, Y.-J., Cheng, M.-Y., Chang, W.-Y., Tsao, L.-C., Yang, S.-A., Shih, W.-P., Chang, F.-Y., Chang, S.-H., and Fan, K.-C. (2008) An integrated flexible temperature and tactile sensing array using PI–copper films. *Sensors and Actuators A*, **143**, 143–153.

84 Yang, Y.-J., Cheng, M.-Y., Shih, S.-C., Huang, X.-H., Tsao, C.-M., Chang, F.-Y., and Fan, K.-C. (2010) A 32 × 32 temperature and tactile sensing array using PI–copper films. *International Journal of Advanced Manufacturing Technology*, **46**, 945–956.

85 Cirillo, A., Cirillo, P., De Maria, G., Natale, C., and Pirozzi, S. (2014) An artificial skin based on optoelectronic technology. *Sensors and Actuators A*, **212**, 110–122.

86 Seminara, L., Capurro, M., and Valle, M. (2015) Tactile data processing method for the reconstruction of contact force distributions. *Mechatronics*, **27**, 28–37

87 Arabshahi, S.A. and Jiang, Z. (2005) Development of a tactile sensor for Braille pattern recognition: sensor design and simulation. *Smart Materials and Structures*, **14**, 1569–1578.

88 Decherchi, S., Gastaldo, P., Dahiya, R.S., Valle, M., and Zunino, R. (2011) Tactile-data classification of contact materials using computational intelligence. *IEEE Transactions on Robotics*, **37** (3), 635–639.

89 Kim, S.H., Engel, J., Liu, C., and Jones, D.L. (2005) Texture classification using a polymer-based MEMS tactile sensor. *Journal of Micromechanics and Microengineering*, **15** (5), 912–920.

90 Hosoda, K., Tada, Y., and Asada, M. (2006) Anthropomorphic robotic soft fingertip with randomly distributed receptors. *Robotics and Autonomous Systems*, **54**, 104–109.

91 Jamali, N. and Sammut, S. (2011) Majority voting: material classification by tactile sensing using surface texture. *IEEE Transactions on Robotics*, **27**, 508–521.

92 Maheshwari, V. and Saraf, R.F. (2006) High-resolution thin-film device to sense texture by touch. *Science*, **312** (5779), 501–1504.

93 Sinapov, J., Sukhoy, V., Sahai, R., and Stoytchev, A. (2011) Vibrotactile recognition and categorization of surfaces by a humanoid robot. *IEEE Transactions on Robotics*, **27** (3), 488–497.

94 Oddo, C.M., Controzzi, M., Beccai, L., Cipriani, C., and Carrozza, M.C. (2011) Roughness encoding for discrimination of surfaces in artificial active-touch. *IEEE Transactions on Robotics*, **27** (3), 522–533.

95 Francomano, M.T., Accoto, D., and Guglielmelli, E. (2013) Artificial sense of slip: a review. *IEEE Sensors Journal*, **13** (7), 2489–2498.

96 Najarian, S., Dargahi, J., and Mehrizi, A. (2009) *Artificial Tactile Sensing in Biomedical Engineering*, McGraw Hill Professional.

97 Ho, A. and Hirai, S. (2014) *Mechanics of Localized Slippage in Tactile Sensing: And Application to Soft Sensing Systems*, Springer Tracts in Advanced Robotics, vol. 99, Springer International Publishing, Cham, Switzerland.

98 Romano, J.M., Hsiao, K., Niemayer, G., Chitta, S., and Kuchenbecker, K.J. (2011) Human-inspired robotic grasp control with tactile sensing. *IEEE Transactions on Robotics*, **99**, 1–13.

99 Cooney, M.D., Nishio, S., and Ishiguro, H. (2014) Importance of touch for conveying affection in a multimodal interaction with a small humanoid robot. *International Journal of Humanoid Robotics*, **12**. doi: 10.1142/S0219843615500024

100 Tawil, D.S., Rye, D., and Velonaki, M. (2012) Interpretation of the modality of touch on an artificial arm covered with an EIT-based sensitive skin. *International Journal of Robotics Research*, **31**, 1627–1641.

101 Gastaldo, P., Pinna, L., Seminara, L., Valle, M., and Zunino, R. (2014) A tensor-based pattern recognition framework for the interpretation of touch modality in artificial skin systems. *IEEE Sensors Journal*, **14** (7), 2216–2225.

102 Stiehl, W.D. and Breazeal, C. (2005) Affective touch for robotic companions, affective computing and intelligent interaction. *Lecture Notes in Computer Science*, **3784**, 747–754.

103 Yohanan, S. and MacLean, K. (2012) The role of affective touch in human–robot interaction: human intent and expectations in touching the haptic creature. *International Journal of Social Robotics*, **4**, 163–180.

104 Cutkosky, M.R., Howe, R.D., and Provancher, W. (2007) Force and tactile sensors, in *Springer Handbook of Robotics*, Springer, Berlin, pp. 455–476.

105 De Rossi, D., Caiti, A., Bianchi, R., and Canepa, G. (1991) Fine-form tactile discrimination through inversion of data from a skin-like sensor. Proceedings of the 1991 IEEE International Conference on Robotics and Automation, Sacramento, CA, pp. 398–403.

106 Cranny, A., Cotton, D.P.J., Chappell, P.H., Beeby, S.P., and White, N.M. (2005) Thick-film force, slip and temperature sensors for a prosthetic hand. *Measurement Science and Technology*, **16**, 1–11.

107 Cranny, A., Cotton, D.P.J., Chappell, P.H., Beeby, S.P., and White, N.M. (2005) Thick-film force and slip sensors for a prosthetic hand. *Sensors and Actuators A*, **123–124**, 162–171.

108 Howe, R.D. and Cutkosky, M.R. (1989) Sensing skin acceleration for slip and texture perception. Proceedings on the IEEE International Conference on Robotics and Automation, pp. 145–150.

109 Mingrino, A., Bucci, A., Magni, R., and Dario, P. (1994) Slippage control in hand prostheses by sensing grasping forces and sliding motion. *Proceedings of the IEEE/RSJ International Conference on Intelligent Robots and Systems*, **3** (3), 1803–1809.

110 Scholkopf, B. and Smola, A.J. (2001) *Learning with Kernels*, MIT Press, Cambridge, MA.

111 Goger, D., Gorges, N., and Worn, H. (2009) Tactile sensing for an anthropomorphic robotic hand: hardware and signal processing. Proceedings of the IEEE International Conference on Robotics and Automation, Kobe, Japan, May 12–17, pp. 895–901.

112 Silvester, P. and Ferrary, R. (1996) *Finite Elements for Electrical Engineers*, 3rd edn, Cambridge University Press, Cambridge, UK.

113 Lionheart, W., Polydorides, N., and Borsic, A. (2005) The reconstruction problem, in *Electrical Impedance Tomography: Methods, History and Applications* (ed. D.S. Holder), Institute of Physics, Bristol, UK, pp. 3–63.

114 Adler, A. and Guardo, R. (1996) Electrical impedance tomography: regularized imaging and contrast detection. *IEEE Transactions on Medical Imaging*, **15** (2), 170–179.

115 Adler, A. and Lionheart, W.R.B. (2006) Uses and abuses of EIDORS: an extensible software base for EIT. *Physiological Measurement*, **27**, S25–S42.

116 Signoretto, M., De Lathauwerb, L., and Suykens, J.A.K. (2011) A kernel based framework to tensorial data analysis. *Neural Network*, **24** (8), 861–874.

117 Zhao, Q., Zhou, G., Adali, T., Zhang, L., and Cichocki, A. (2013) Kernelization of tensor-based models for multiway data analysis: processing of multidimensional structured data. *IEEE Signal Processing Magazine*, **30** (4), 137–148.